Clinical and Translational Radiation Oncology 20 (2020) 53–57

Contents lists available at ScienceDirect

Clinical and Translational Radiation Oncology

journal homepage: www.elsevier.com/locate/ctro

Original Research Article

A model system for studying superselective radiotherapy of lymph node metastasis in mice with swollen lymph nodes

Ryohei Kikuchi [a,b], Ariunbuyan Sukhbaatar [a,b,c], Maya Sakamoto [d], Shiro Mori [a,b,e], Tetsuya Kodama [a,b,*]

[a] Laboratory of Biomedical Engineering for Cancer, Graduate School of Biomedical Engineering, Tohoku University, 4-1 Seiryo, Aoba, Sendai, Miyagi 980-8575, Japan
[b] Biomedical Engineering Cancer Research Center, Graduate School of Biomedical Engineering, Tohoku University, 4-1 Seiryo, Aoba, Sendai, Miyagi 980-8575, Japan
[c] Department of Oral and Maxillofacial Surgery, Graduate School of Dentistry, Tohoku University, 1-1 Seiryo, Aoba, Sendai, Miyagi 980-8575, Japan
[d] Department of Oral Diagnosis, Tohoku University Hospital, 1-1 Seiryo, Aoba, Sendai, Miyagi 980-8574, Japan
[e] Department of Oral and Maxillofacial Surgery, Tohoku University Hospital, 1-1 Seiryo, Aoba, Sendai, Miyagi 980-8574, Japan

ARTICLE INFO

Article history:
Received 5 February 2019
Revised 24 April 2019
Accepted 15 May 2019
Available online 18 May 2019

Keywords:
Radiation
Mouse model
Lymph node
Metastasis
Abscopal effect

ABSTRACT

Utilizing mice with swollen lymph nodes, we succeeded in irradiating individual metastatic lymph nodes through a hole in a lead shield. This system enabled us to increase the radiation dose to >8 Gy (the lethal dose for total-body irradiation) and evaluate both direct and abscopal antitumor effects.

It is not possible for ethical reasons to resect lymph nodes (LNs) from patients during the course of radiotherapy for metastatic LNs (MLNs) or carry out histopathological examinations over time. Thus, the effect of radiation on the histopathology of MLNs has remained unclear. The normal mouse LN is about 1–2 mm in diameter [1], making it difficult to selectively irradiate individual LNs without imaging modalities with high-resolution or surgically making an incision of the mouse body when mice are used in pathology-based studies of MLN radiotherapy. Therefore, most previous investigations have used whole-body irradiation for experimental radiotherapy of mice. Since 8 Gy of total body irradiation corresponds to a lethal dose [2–4], it has been difficult to investigate the effects of irradiation on an individual LN.

LN metastasis occurs when tumor cells invade from the afferent lymphatic vessels into the marginal sinus, where they proliferate [1,5,6]. In normal mice, the size of a LN is about 1 to 2 mm along the major axis [1]. Due to its small size, a mouse LN exhibits extranodal invasion or is replaced by metastatic tumor during the early stages of nodal metastasis. Consequently, the pathological features of MLNs in mice will likely be very different from those of MLNs in humans, limiting the usefulness of models based on normal mice.

In previous studies, we have developed a LN metastasis model using MXH10/Mo-*lpr/lpr* (MXH10/Mo/lpr) mice, which have LNs of comparable size to those found in humans [7–9]. In this metastasis model, the injection of luciferase (Luc)-expressing tumor cells into the subiliac LN (SiLN) forms a metastatic lesion in the ipsilateral proper axillary LN (PALN), which tumor cells reach via lymphatic vessels connecting the two LNs. The process of LN metastasis formation can be monitored *in vivo* using a bioluminescence imaging system [5,10–12]. An advantage of our experimental mice is that the superficial SiLN and PALN are enlarged to about 10 mm in size, which permits shielding of sites other than the target LN with a lead plate. Long-term survival of the animal is possible even after irradiation of a LN with an X-ray dose $\geq$8 Gy, which is normally lethal to mice when given as whole-body irradiation. Consequently, an irradiated LN can be analyzed in real time for a long period using bioluminescence imaging or high-frequency ultrasound imaging with enhanced contrast.

Radiation therapy also evokes an abscopal effect, whereby an irradiated tumor induces the weakening of non-irradiated metastatic cells at a site distant to it, and this phenomenon is known to involve cancer immunity mechanisms [13]. Previous studies in

* Corresponding author at: Laboratory of Biomedical Engineering for Cancer, Graduate School of Biomedical Engineering, Tohoku University, 4-1 Seiryo, Aoba, Sendai, Miyagi 980-8575, Japan.
E-mail address: kodama@tohoku.ac.jp (T. Kodama).

https://doi.org/10.1016/j.ctro.2019.05.002

mice have shown that CD8-positive lymphocytes are necessary for tumor regression and extension of survival following irradiation, and it has been reported that anti-tumor immunity is enhanced by the administration of anti-CTLA-4 antibody as an immune checkpoint inhibitor [14]. It is expected that a treatment for LN metastasis based on immunoradiotherapy and an immune checkpoint inhibitor will be developed in the near future. However, designing experiments to analyze how the abscopal effect is influenced by the stage of LN metastasis and the irradiation dose has been difficult to achieve using previous models of LN metastasis. Our model based on MXH10/Mo/lpr mice allows the observation of LN metastasis over time from initiation of the process as well as variation of experimental conditions such as the dose, exposure number and timing of irradiation. In this paper, we report a unique experimental model for studying the radiation-induced abscopal effects. This model system is based on MXH10/Mo/lpr mice, which have LNs of comparable size to those in humans.

1. Experimental animals

MXH10/Mo/lpr mice [7] were used ($n = 18$, aged 14 to 15 weeks). The Institutional Animal Care and Use Committee of Tohoku University accepted our research protocols.

MXH10/Mo-*lpr*/*lpr* (MXH10/Mo/lpr) mice are a congenic strain of MRL/Mp-*lpr*/*lpr* (H-2^k haplotype) and C3H/HeJ-*lpr*/*lpr* (H-2^k haplotype) mice. The LNs enlarge to about 10 mm in diameter at 12 weeks of age due to invasion by *lpr*-T ($CD4^-CD8^-B220^+Thy^+$) cells, which are accumulated in the paracortical region. Since the *lpr* gene is a *fas*-deletion mutant gene, MXH10/Mo/lpr mice do not express the *fas* gene involved in apoptosis. Thus, the immune system in MXH10/Mo/lpr mice is functional except for the signaling pathway related to *fas*. In addition, anatomical structures in MXH10/Mo/lpr mice are same as those in wild-type mice. In general, mice have two types of LN in their axillary regions: a PALN and an accessory axillary LN (AALN). The PALN is downstream of both the AALN and SiLN in the mouse lymphatic system. The flow characteristics of the lymphatic vessels and blood vessels that run between the PALN and SiLN in MXH10/Mo/lpr mice are similar to those of C57BL/6J and BALB/c mice [7].

2. Cell culture

FM3A-Luc cells (C3H/He mouse mammary carcinoma cells expressing the luciferase gene) [7] have an H-2^k haplotype, which is the same as that of MXH10/Mo/lpr mice, and expressed vascular endothelial growth factor (VEGF)-A and VEGF-B but not VEGF-C. The relative growth rates of FM3A-Luc cells was 1.1/day {Kodama, 2018 #6}. Cells were cultured in RPMI-1640 medium containing 10% (v/v) fetal bovine serum, 1% (v/v) L-glutamine-penicillin–streptomycin (all from Sigma-Aldrich, USA), and 0.5 mg/mL Geneticin G418 (FujiFilm Wako Pure Chemical Co., Japan). Cells were maintained in a culture incubator under a 5% CO_2 atmosphere at 37 °C.

3. Induction of LN metastasis

Eighteen mice were divided into two groups, namely a control group (normal PALN exposed to radiation; $n = 4$) and a metastasis group (metastatic PALN with radiation; $n = 14$). Please note that the PALN and AALN were irradiated through a hole in the lead shield as described below. In the metastasis group, a 60-μL aliquot of tumor cells (3.3×10^5 cells/mL in phosphate-buffered saline and 1:2 v/v Matrigel) was manually injected into the SiLN to produce metastasis in the PALN. The tumor inoculation day was defined as day 0 [12]. Tumor progression in the PALN and SiLN was evaluated from measurements of luciferase activity with an IVIS Lumina bioluminescence system (PerkinElmer, USA) on day 0, day 7, day 14, day 21 and day 28.

4. X-ray irradiation of regional LNs

Metastasis was deemed to have occurred in the PALN when luciferase activity exceeded the background level of the control (1×10^6 photons/s), and this time point was defined as day 0^T. The metastatic PALN was exposed to X-ray radiation on day^T. A lead shield made from 2 identical lead plates (thickness: 2 mm; hole diameter: 2 cm; size, 17 cm × 13 cm) was positioned on the mouse (Fig. 1A) so that the AALN and PALN in the axillary region were exposed to 8 Gy of X-ray radiation (0.72 Gy/min) through the hole in the lead shield (Fig. 1B). The X-rays were emitted from an irradiation device (tube voltage: 200 kV; tube current: 10 mA; PANTAK, Shimadzu Co., Japan). The control group (tumor inoculation into the SiLN not performed) was irradiated under the same conditions. The radiation dose to other body regions was reduced to 0.008 Gy by the lead shield, preventing X-ray-induced biological effects in regions other than the PALN and AALN.

5. Evaluation of radiation-induced antitumor effects in the PALN

Radiation-induced anti-tumor effects in the PALN were evaluated from measurements of luciferase activity with an IVIS (PerkinElmer) on day 0^T, day 3^T, day 6^T, and day 9^T. If tumor cells in the PALN had been detected at day 28, the maximum day of evaluation would have been day 9^T, i.e., day 37 after inoculation of tumor cells into the SiLN. Considering the tumor size in the SiLN and the ethical guidelines in our university, a maximum evaluation day was set to day 9^T.

6. Histological studies

The SiLN and PALN were removed on day 9^T and embedded in paraffin blocks, which were cut into 3-μm sections and stained with hematoxylin and eosin. The SiLN (4 of 14 mice) and PALN (4 of 14 mice) were removed on day 9^T and embedded in paraffin blocks, which were cut into 3-μm sections and stained with hematoxylin and eosin. The specimen was measured under magnification (×40 or ×100) using a microscope (BX51; Olympus Co.) and digital camera (DP72; Olympus).

7. Results and discussion

Most previous investigations using mice have used whole-body irradiation to irradiate LNs because normal mouse LN are about 1 to 2 mm in diameter [1], making it difficult to irradiate selectively individual LNs. In addition, a maximum single-dose-radiation is less than 8 Gy that corresponds to a lethal dose [2–4]. In the present study, we exhibit a mouse model in which a single-dose-radiation ≥8 Gy targets a single LN. First, we investigated the macroscopic changes following irradiation of the PALN and AALN in the axillary region (Fig. 1C). After exposure to 8 Gy of X-rays on day 0^T, the PALN and AALN exhibited a time-dependent decrease in volume. Macroscopic skin damage was not observed for either LN.

Next, we investigated X-ray-induced antitumor effects in the metastatic PALN. Metastasis in the PALN was induced by the

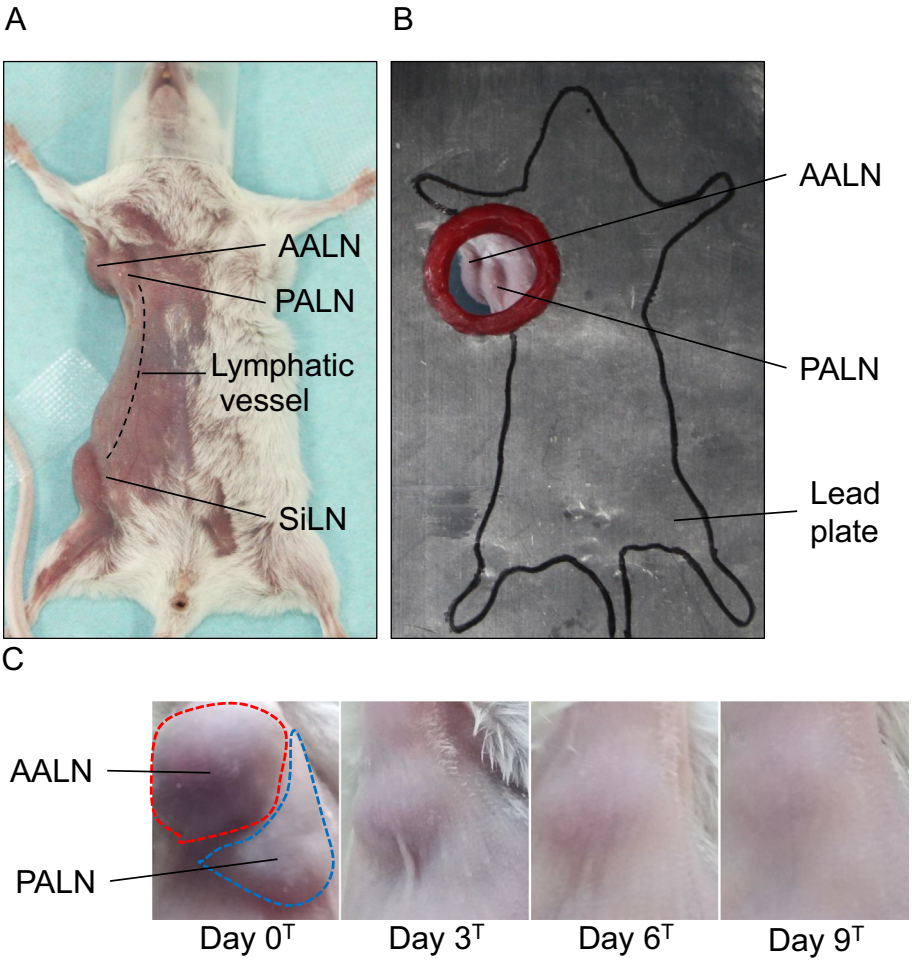

Fig. 1. Protection of the mouse body from irradiation using a lead shield. A. Positioning of the mouse. The mouse was fixed in a supine position with surgical tape to prevent deviation due to breathing during radiotherapy. SiLN: subiliac lymph node, PALN: proper axillary lymph node, AALN: accessory axillary lymph node. Lymphatic vessels connect the SiLN and PALN. The tail was fixed with surgical tape and covered by the lead shield. B. Placement of the lead shield. The lead shield was positioned so that the PALN and AALN were exposed to radiation from the hole. The shield was made from 2 identical lead plates (thickness: 2 mm; hole diameter: 2 cm; size, 17 cm × 13 cm). C. Changes in the volumes of the AALN and PALN as a function of time after exposure to radiation. The day when both lymph nodes were exposed to X-rays was defined as day 0^T ($n = 4$). The volumes of both lymph nodes decreased with time (in days) after irradiation. Irradiation did not produce any detectable macroscopic skin damage.

injection of tumor cells into the SiLN (Fig. 2A). Luciferase signals in the PALN indicative of metastasis were detected on day 7 (Fig. 2B), and luciferase activity in the PALN increased rapidly after day 14. After irradiation of the PALN on day 0^T, the increase in luciferase activity in the PALN was inhibited (Tukey test: day 0^T–day 9^T; day 0^T *vs* day 6^T, $^{**}P = 0.006$).

We further evaluated whether irradiation of the PALN and AALN induced an abscopal effect in the SiLN. Luciferase activity in the SiLN increased steadily from day 0 (Fig. 2B). The first fluorescence signals in the SiLN were detected on day 7 (Fig. 2A). After irradiation on day 0^T, the increase in luciferase activity in the SiLN was attenuated (Fig. 2B). Inhibition of the increase in luciferase activity in a SiLN not exposed to X-rays indicated the presence of an abscopal effect.

Fig. 3 shows histological results of the PALN and SiLN on day 9^T. In PALN irradiated with 8 Gy, intercellular spaces were observed between tumor cells that infiltrated and proliferated into the lymphatic sinuses. Karyomegaly, karyopyknosis, karyorrhexis, apoptotic body, karyolysis, etc. were observed in tumor cells. While, in the SiLN (tumor inoculation site, without radiation), infiltration and proliferation of tumor cells were observed. Similarly, karyomegaly, karyopyknosis, karyorrhexis, apoptotic body, karyolysis, etc. were observed in tumor cells. In addition, a large region of necrosis was observed. It is unclear whether the formation of this necrosis region was due to ischemia caused by rapidly growing tumor or the abscopal effect that resulted from radiation of the PALN.

This novel system enables metastatic LNs to be treated with large single doses of X-ray irradiation (≥8 Gy) as well as multiple-fraction radiotherapy and could be tailored for use in the clinical setting.

MXH10/Mo/lpr mice do not express the *fas* gene involved in apoptosis. Thus, the immune system in MXH10/Mo/lpr mice is functional except for the signaling pathway related to *fas*. Recently, an abscopal effect was confirmed in patients with malignant melanoma who were treated with both radiation and immune checkpoint inhibitor therapy [15], suggesting that immune checkpoint inhibition facilitates the expression of the abscopal effect by activating tumor-specific lymphocytes [13]. We anticipate that further research with this system will help to elucidate in detail the mechanism(s) involved in the activation of systemic antitumor immunity by localized irradiation.

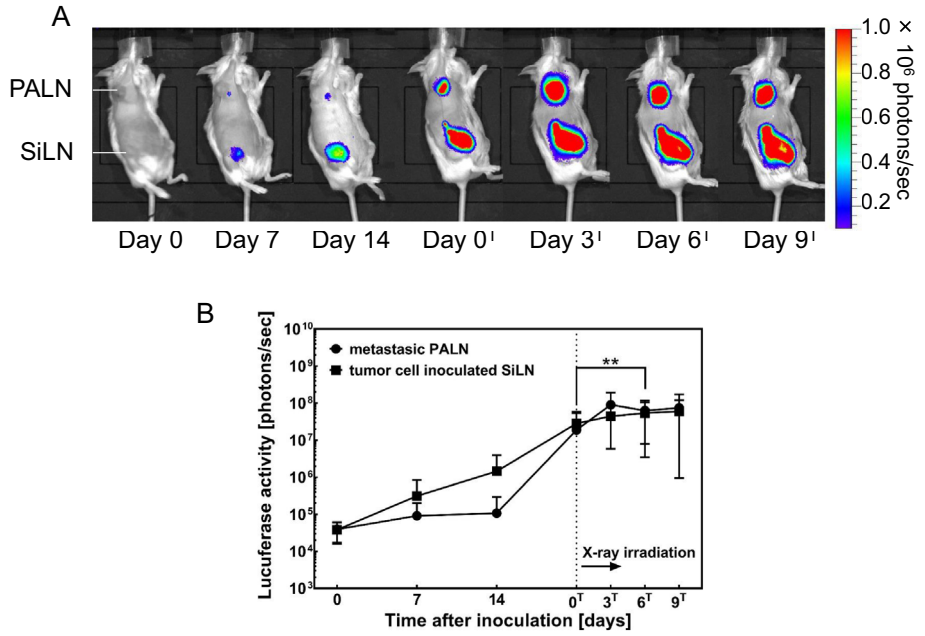

Fig. 2. Bioluminescence imaging. Bioluminescence images. Metastasis was induced in the PALN by inoculation of the SiLN with tumor cells on day 0 (n = 14). Metastasis was detected in the PALN from day 7. Luciferase activity in the center of the SiLN decreased from day 6^T to day 9^T. B. Alterations in luciferase activity in the PALN. Luciferase activity increased rapidly after day 14 and was inhibited by X-ray irradiation on day 0^T (n = 14) (Tukey test: PALN [day 0^T–day 9^T]; day 0^T *vs* day 6^T, $^{**}P$ = 0.006). Luciferase activity in the SiLN increased steadily and was inhibited from day 0^T, indicating that an abscopal effect was induced in the SiLN (n = 14). Mean ± SEM.

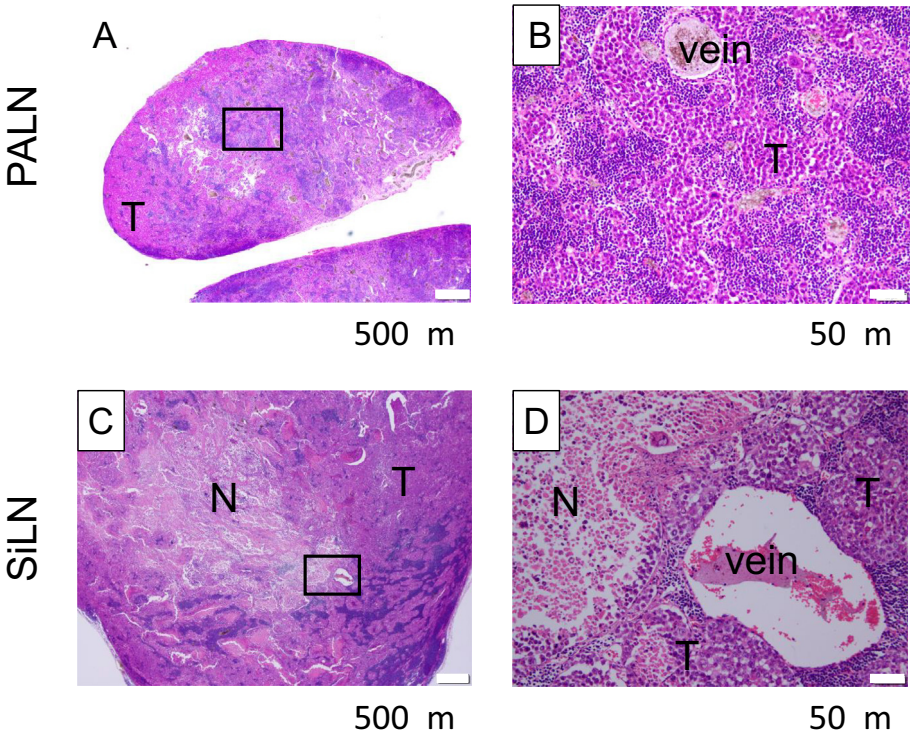

Fig. 3. Histological analysis (HE staining) of the X-ray-irradiated PALN and SiLN shield with a lead plate on day 9^T. (A, B): PALN exposure to X-rays (8 Gy) at day 0^T, obtained on day 9^T. (C, D): SiLN shield with a lead plate, obtained on day 9^T. Tumor cells were inoculated into the SiLN to induce metastasis in the PALN. The metastatic PALN was exposed to X-ray radiation on day^T. PALN and SiLN were obtained on day 9^T. Boxes (A, C) outline the magnified view shown in (B, D). In PALN irradiated with 8 Gy, intercellular spaces were observed between tumor cells that infiltrated and proliferated into the lymphatic sinuses. Karyomegaly, karyopyknosis, karyorrhexis, apoptotic body, karyolysis, etc. were observed in tumor cells. In the SiLN (tumor inoculation site, without radiation), infiltration and proliferation of tumor cells were observed. Karyomegaly, karyopyknosis, karyorrhexis, apoptotic body, karyolysis etc. were observed in tumor cells. In addition, large necrosis region was observed. T: tumor, N: necrosis. Scale bars (A, B): 500 μm. Scale bars (C, D): 50 μm.

Acknowledgements

The present research was funded by JSPS KAKENHI with grants to TK (17H00865 and 17K20077) and MS (18H03544). The authors would like to thank the Biomedical Research Core of Tohoku University Graduate School of Medicine for invaluable technical support and T. Sato for excellent technical assistance.

Contributions

The present research was designed by RK, SM and TK. The experiments were carried out by RK and AS. The manuscript was written and figures created by RI, AS, SM and TK. All authors contributed to data interpretation and were equally involved in reviewing the final submitted manuscript.

Statement of potential competing financial interests

The authors declare that there are no competing financial interests.

Appendix A. Supplementary data

Supplementary data to this article can be found online at https://doi.org/10.1016/j.ctro.2019.05.002.

References

[1] Takeda T, Mori S, Kodama T. Study of fluid dynamics reveals direct communications between lymphatic vessels and venous blood vessels at lymph nodes of mice. J Immunol Methods 2017;445:1–9.
[2] Paris F, Fuks Z, Kang A, Capodieci P, Juan G, Ehleiter D, et al. Endothelial apoptosis as the primary lesion initiating intestinal radiation damage in mice. Science 2001;293:293–7.
[3] Kushida T, Inaba M, Takeuchi K, Sugiura K, Ogawa R, Ikehara S. Treatment of intractable autoimmune diseases in MRL/lpr mice using a new strategy for allogeneic bone marrow transplantation. Blood 2000;95:1862–8.
[4] Takeuchi K, Inaba M, Miyashima S, Ogawa R, Ikehara S. A new strategy for treatment of autoimmune diseases in chimeric resistant MRL/lpr mice. Blood 1998;91:4616–23.
[5] Shao L, Takeda K, Kato S, Mori S, Kodama T. Communication between lymphatic and venous systems in mice. J Immunol Methods 2015;124:100–5.
[6] Kodama T, Mori S, Nose M. Tumor cell invasion from the marginal sinus into extranodal veins during early-stage lymph node metastasis can be a starting point for hematogenous metastasis. J Cancer Metastasis Treat 2018;4:56.
[7] Shao L, Mori S, Yagishita Y, Okuno T, Hatakeyama Y, Sato T, et al. Lymphatic mapping of mice with systemic lymphoproliferative disorder: usefulness as an inter-lymph node metastasis model of cancer. J Immunol Methods 2013;389:69–78.
[8] Tanaka Y, Komori H, Mori S, Soga Y, Tsubaki T, Terada M, et al. Evaluating the role of rheumatoid factors for the development of rheumatoid arthritis in a mouse model with a newly established ELISA system. Tohoku J Exp Med 2010;220:199–206.
[9] Nose M, Komori H, Miyazaki T, Mori S. Genomics of vasculitis: lessons from mouse models. Ann Vasc Dis 2013;6:16–21.
[10] Kodama T, Hatakeyama Y, Kato S, Mori S. Visualization of fluid drainage pathways in lymphatic vessels and lymph nodes using a mouse model to test a lymphatic drug delivery system. Biomed Opt Express 2015;6:124–34.
[11] Okuno T, Kato S, Hatakeyama Y, Okajima J, Maruyama S, Sakamoto M, et al. Photothermal therapy of tumors in lymph nodes using gold nanorods and near-infrared laser light. J Controlled Release 2013;172:879–84.
[12] Tada A, Horie S, Mori S, Kodama T. Therapeutic effect of cisplatin given with a lymphatic drug delivery system on false-negative metastatic lymph nodes. Cancer Sci 2017;108:2115–21.
[13] Liu Y, Dong Y, Kong L, Shi F, Zhu H, Yu J. Abscopal effect of radiotherapy combined with immune checkpoint inhibitors. J Hematol Oncol 2018;11:104.
[14] Yoshimoto Y, Suzuki Y, Mimura K, Ando K, Oike T, Sato H, et al. Radiotherapy-induced anti-tumor immunity contributes to the therapeutic efficacy of irradiation and can be augmented by CTLA-4 blockade in a mouse model. PLoS One 2014;9:e92572.
[15] Grimaldi AM, Simeone E, Giannarelli D, Muto P, Falivene S, Borzillo V, et al. Abscopal effects of radiotherapy on advanced melanoma patients who progressed after ipilimumab immunotherapy. Oncoimmunology 2014;3:e28780.